Inclusive charm production in $\Upsilon(nS)$ decay

Daekyoung Kang,[1,2] Taewon Kim,[1] Jungil Lee,[1,2] and Chaehyun Yu[1]

[1]*Department of Physics, Korea University, Seoul 136-701, Korea*
[2]*Physics Department, Ohio State University, Columbus, Ohio 43210, USA*

Based on the nonrelativistic QCD (NRQCD) factorization formalism, we calculate the inclusive charm production rate in $\Upsilon(nS)$ decay at leading order in the strong coupling constant α_s and the relative velocity v of the b quark in the quarkonium rest frame. The branching fractions for $\Upsilon(nS)$ to charm for $n = 1, 2$, and 3 are all around 7%–9%. About 60% of the branching fraction into charm is from annihilation of the color-singlet $b\bar{b}$ pair into $\gamma^* \to c\bar{c}$. Most of the remaining branching fraction is from annihilation of the color-singlet $b\bar{b}$ pair decaying into $c\bar{c}gg$. We also compute the momentum distributions of the charm quark and charmed hadrons in the decays. The virtual-photon contribution to the charm-quark momentum distribution is concentrated at the end point while the $c\bar{c}gg$ contribution is broad. The momentum distributions for charmed hadrons are obtained by convolving the charm-quark momentum distribution with charm fragmentation functions. This makes the momentum distributions for charmed hadrons softer than that for the charm quark. This effect is particularly significant in the virtual-photon contribution.

I. INTRODUCTION

According to the nonrelativistic QCD (NRQCD) factorization formalism, an annihilation decay rate of a spin-triplet S-wave ($^3S_1$) bottomonium Υ[1] is expressed as an infinite series of NRQCD matrix elements with corresponding short-distance coefficients [1]. The NRQCD matrix elements, which reflect the long-distance nature of the quarkonium, scale as powers of the bottom-quark velocity v in the quarkonium rest frame, which is $v^2 \approx 0.1$. At leading order in v, the inclusive decay rate of the Υ is dominated by the color-singlet spin-triplet contribution whose NRQCD matrix element is $\langle \mathcal{O}_1(^3S_1)\rangle_\Upsilon = \langle\Upsilon|\mathcal{O}_1(^3S_1)|\Upsilon\rangle$, which is defined in Ref. [1]. The subscript 1 on the NRQCD four-quark operator $\mathcal{O}_1$ denotes that it is a color-singlet operator. Thus, at leading order in v, the inclusive light-hadronic decay rate of the Υ is expressed in a factorized form:

$$\Gamma[\Upsilon \to X] = C_1 \frac{\langle \mathcal{O}_1(^3S_1)\rangle_\Upsilon}{m_b^2}, \qquad (1)$$

where X represents all possible light-hadronic final states into which Υ can decay and m_b is the bottom-quark mass. The short-distance coefficient C_1, which is insensitive to the long-distance nature of the Υ, can be calculated perturbatively. The dimension of the matrix element $\langle \mathcal{O}_1(^3S_1)\rangle_\Upsilon$ is 3 so that C_1 is dimensionless.

At leading order in α_s, the dominant color-singlet contribution to C_1 comes from the $b\bar{b}_1(^3S_1) \to ggg$ mode, where the three gluons are attached to the bottom-quark line. Here, α_s is the strong coupling constant and $b\bar{b}_1(^{2s+1}L_J)$ is the color-singlet $b\bar{b}$ pair with spin s, orbital

angular momentum L, and total angular momentum J. The leading contribution of order α_s^3 to C_1 is known through the orthopositronium decay rate obtained by Caswell, Lepage, and Sapirstein [2]. The order-α_s^4 corrections to C_1 were calculated by Mackenzie and Lepage [3]. This result was confirmed recently by Campbell, Maltoni, and Tramontano [4].

In addition to the three-gluon mode, C_1 may include the virtual-photon contribution from $b\bar{b}_1(^3S_1) \to \gamma^* \to q\bar{q} + X$. The decay rate is of order $e_b^2 e_q^2 \alpha^2$, where α is the QED coupling constant and e_q is the fractional electric charge of the quark q: $e_q = \frac{2}{3}$ for an up-type quark and $-\frac{1}{3}$ for a down-type quark. That electromagnetic decay rate may appear to be highly suppressed compared to the three-gluon mode of order α_s^3. However, we can make a rough estimate of the branching fraction $\text{Br}[\Upsilon \to \gamma^* \to q\bar{q}]$ by using the measured branching fractions for $\text{Br}[\Upsilon \to e^+ e^-]$ [5]: $\text{Br}[\Upsilon \to \gamma^* \to q\bar{q}] \approx N_c \text{Br}[\Upsilon \to e^+ e^-]\sum_q e_q^2$, where the sum is over the four flavors of quarks lighter than the bottom and $N_c = 3$ is the number of colors. According to this estimate, $\text{Br}[\Upsilon \to \gamma^* \to q\bar{q}] \approx 6\%$–8%, which may not be negligible.

At higher orders in v, the NRQCD factorization formula (1) must include additional contributions from higher Fock states which involve color-octet pairs $b\bar{b}_8(^{2s+1}L_J)$ as well as the color-singlet ones, which are suppressed compared to the leading contribution in Eq. (1). The order-v^2 and order-v^4 relativistic corrections to the color-singlet contributions were calculated by Keung and Muzinich [6] and by Bodwin and Petrelli [7], respectively. Some of the color-octet contributions were also calculated in Refs. [8–10].

Because the Υ is heavy enough, the decay products may include a pair of charmed hadrons. However, unlike the light-hadronic decay mode of the Υ, there has been little previous work on open-charm production in Υ decay. In 1978, Fritzsch and Streng predicted the branching fraction

---

[1]Throughout this paper, we suppress the identifier nS in $\Upsilon(nS)$, where n is the radial quantum number, unless it is necessary.

of the decay of Υ into charm to be a few percents [11], where they considered $\Upsilon \rightarrow ggg^*$ followed by $g^* \rightarrow c\bar{c}$. In 1979, Bigi and Nussinov took into account a fusion process $\Upsilon \rightarrow c\bar{c}g$ of order α_s^5, in which a pair of virtual gluons create the $c\bar{c}$ pair [12]. In 1992, ARGUS experiment searched for charm production in direct decays of the $\Upsilon(1S)$ to find only an upper limit of $\text{Br}^{\text{dir}}[\Upsilon(1S) \rightarrow D^*(2010)^\pm + X] < 0.019$ [13].

Recent runs of the CLEO III experiment have produced a large amount of data samples at the $\Upsilon(1S)$, $\Upsilon(2S)$, and $\Upsilon(3S)$ resonances. The B-factory experiments *BABAR* and Belle have accumulated data for $\Upsilon(2S)$ and $\Upsilon(3S)$ provided by initial-state radiation. The Belle Collaboration has also collected data by running on the $\Upsilon(3S)$ resonance. With these high-luminosity data, one can now indeed study open-charm production in Υ decay. Very recently, some of the authors have calculated the total production rates and momentum distributions of the charm quark and charmed hadrons, respectively, in the P-wave bottomonium decays $\chi_{bJ} \rightarrow c + X$ for $J = 0$, 1, and 2 by using the NRQCD factorization formalism [14]. In order to calculate the momentum distribution of the charmed hadrons they used the momentum distribution of charmed hadrons measured by the Belle Collaboration in e^+e^- annihilation [15].

In this work, as an extension of a previous study [14], we consider inclusive charm production in the spin-triplet S-wave bottomonium decay. At leading order in v, the dominant mechanism for the decay is a color-singlet channel $b\bar{b}_1(^3S_1) \rightarrow ggg^*$ followed by $g^* \rightarrow c\bar{c}$. As we have described earlier, the color-singlet mode may have significant virtual-photon contribution from $b\bar{b}_1(^3S_1) \rightarrow \gamma^*$ followed by $\gamma^* \rightarrow c\bar{c}$. For inclusive charm production, the virtual-photon contribution may have a larger fraction than that in the inclusive light-hadronic decay because the rate for $\Upsilon \rightarrow c\bar{c}gg$ is suppressed by order α_s compared to that for $\Upsilon \rightarrow ggg$. We consider the virtual-photon contribution as well as the QCD contributions from $b\bar{b}_1(^3S_1) \rightarrow c\bar{c}gg$ and $b\bar{b}_1(^3S_1) \rightarrow c\bar{c}g\gamma$ modes. In the current CLEO III analysis on the charmed-hadron (h) momentum distribution in Υ decay, the virtual-photon contribution is subtracted experimentally [16]. We therefore also present the results for the QCD contributions after excluding the virtual-photon process.

This paper is organized as follows. In Sec. II, we present the NRQCD factorization formulas for the inclusive charm production rate and charm-momentum distribution in the spin-triplet S-wave bottomonium decay. We also discuss the NRQCD matrix element that appears as a long-distance factor in the factorization formula. We calculate the charm-quark momentum distribution and the total rate for inclusive charm production in the decay in Sec. III. In Sec. IV, in order to provide a theoretical prediction that can be compared with CLEO III data, we illustrate the charmed-hadron momentum distributions which are obtained by convolving the charm-quark momentum distribution with

fragmentation functions for $c \rightarrow h$ that have been fit to e^+e^- annihilation data. Finally, a brief summary of this work is given in Sec. V.

II. CHARM-QUARK PRODUCTION IN Υ DECAY

In this section, we summarize the NRQCD factorization formula for inclusive charm production in Υ decay. In many aspects there is a large overlap with the formalism for calculating the inclusive charm production rate in the P-wave bottomonium decay [14]. In this work, we follow the same strategies that were employed in Ref. [14]. For details of the formalism, we refer the reader to Refs. [1,14].

A. NRQCD factorization formula

At leading order in v, the NRQCD factorization formula for the inclusive charm production rate in Υ decay has an analogous form to that for the light-hadronic decay in Eq. (1):

$$\Gamma[\Upsilon \rightarrow c + X] = C_1^{(c)} \frac{\langle \mathcal{O}_1(^3S_1) \rangle_\Upsilon}{m_b^2}, \tag{2}$$

where $C_1^{(c)}$ is a dimensionless short-distance coefficient that depends on the mass ratio m_c/m_b of the charm quark and the bottom quark and $c + X$ represents all possible states containing a charmed hadron, such as D^+, D^0, D_s^+, Λ_c^+, or their excited states.

At leading order in v and α_s, the dominant source of $C_1^{(c)}$ is the decay of a $b\bar{b}_1(^3S_1)$ pair into ggg^*, followed by $g^* \rightarrow c\bar{c}$. One of six Feynman diagrams of the process is shown in Fig. 1 and the remaining five diagrams are obtained by permuting the three gluons attached to the bottom-quark line. The decay of a $b\bar{b}_1(^3S_1)$ pair into γgg^*, followed by $g^* \rightarrow c\bar{c}$ also contributes to $C_1^{(c)}$. We call the two processes involving $g^* \rightarrow c\bar{c}$ QCD processes.

Another similar subprocess that has the same final state $c\bar{c}gg$ as the QCD process is the decay of $b\bar{b}_1(^3S_1) \rightarrow gg\gamma^*$ followed by $\gamma^* \rightarrow c\bar{c}$. Because the $c\bar{c}$ pair created in this subprocess is in a color-singlet state, there is no interference between this and the QCD process whose $c\bar{c}$ pair is created in a color-octet state. The contribution of the subprocess $b\bar{b}_1(^3S_1) \rightarrow gg\gamma^*$ followed by $\gamma^* \rightarrow c\bar{c}$ to the Υ decay width is suppressed to the QCD contribution by a
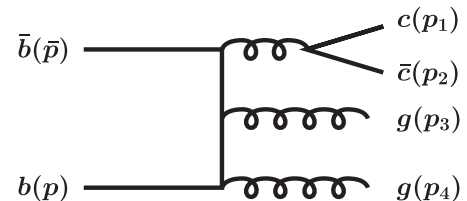

FIG. 1. One of six Feynman diagrams for $b\bar{b} \rightarrow c\bar{c}gg$. The other five diagrams are obtained by permuting the three gluons attached to the bottom-quark line.

multiplicative factor $8e_b^2 e_c^2 \alpha^2 N_c^2 / \alpha_s^2 / (N_c^2 - 4)$. For $\alpha_s(m_\Upsilon/2) \approx 0.215$ and $\alpha(m_\Upsilon/2) \approx 1/132$, the factor is about 0.09%. Therefore, we neglect this subprocess.

In addition to the QCD modes, a virtual-photon mode, $b\bar{b}_1(^3S_1) \to \gamma^*$, followed by $\gamma^* \to c\bar{c} + X$ contributes to $C_1^{(c)}$. A rough estimate of the branching fraction of the virtual-photon channel is about 3%, which is the product of the measured leptonic width $\Gamma[\Upsilon \to e^+ e^-]$, coupling e_c^2, and the color factor N_c. This is comparable to the branching fraction $\mathrm{Br}[\Upsilon \to c\bar{c}gg]$ predicted by Fritzsch and Streng [11]. In this work, we consider the virtual-photon contribution $C_1^{(c/\gamma^*)}$ from $b\bar{b}_1(^3S_1) \to \gamma^* \to c\bar{c}$ as well as the QCD contribution $C_1^{(c/g^*)}$ which is composed of $b\bar{b}_1(^3S_1) \to c\bar{c}gg$ and $b\bar{b}_1(^3S_1) \to c\bar{c}g\gamma$. Then the short-distance coefficient $C_1^{(c)}$ is expressed as

$$C_1^{(c)} = C_1^{(c/g^*)} + C_1^{(c/\gamma^*)}. \tag{3}$$

The two QCD contributions to $C_1^{(c/g^*)}$ are essentially the same except for overall factors so that

$$C_1^{(c/g^*)} = C_1^{(c\bar{c}gg)} + C_1^{(c\bar{c}g\gamma)} = F_\gamma C_1^{(c\bar{c}gg)}, \tag{4}$$

where $C_1^{(c\bar{c}gg)}$ and $C_1^{(c\bar{c}g\gamma)}$ are contributions of $c\bar{c}gg$ and $c\bar{c}g\gamma$ channels to $C_1^{(c/g^*)}$, respectively. The factor F_γ is defined by

$$F_\gamma = 1 + \frac{2e_b^2 \alpha}{\alpha_s} \frac{4N_c}{(N_c^2 - 4)}. \tag{5}$$

For $\alpha_s(m_\Upsilon/2) \approx 0.215$ and $\alpha(m_\Upsilon/2) \approx 1/132$, the numerical value for F_γ is about 1.02, which indicates that the $c\bar{c}g\gamma$ contribution is only about 2% of the QCD contributions. Since we are interested in the total decay rate of $\Upsilon \to c + X$ and distributions of the charm quark with respect to its kinematic variables, we integrate out the phase spaces for the gluons or the photon. Therefore, the total and the differential width of the QCD mode are the same as those for the $c\bar{c}gg$ final state up to the multiplicative factor F_γ in Eq. (5).

As in the case of light-hadronic decay of the Υ, inclusive charm production in Υ decay may have contributions from the decay of the color-octet pair $b\bar{b}_8$ through $b\bar{b}_8 \to g^*$, followed by $g^* \to c\bar{c}$. While the color-octet contribution is suppressed to the color-singlet contribution by order v^4, the short-distance coefficient of the octet process $b\bar{b}_8(^3S_1) \to g^* \to c\bar{c}$ is enhanced by $1/\alpha_s^2$. Therefore, the color-octet channel may have non-negligible contributions, especially for the decay of higher resonances. In this work, we do not consider the color-octet contributions.

In a recent analysis being carried out by the CLEO Collaboration, as a part of experimental measurement, the virtual-photon contribution is subtracted from the data samples of $\Upsilon \to c + X$ by scaling the continuum data by an extra factor based on the branching fractions $\mathrm{Br}[\Upsilon(nS) \to \mu^+ \mu^-]$ and R_{hadrons} but the data include the contribution from $b\bar{b}_1(^3S_1) \to \gamma gg^*$ followed by $g^* \to c\bar{c}$ [16]. The CLEO III data should, therefore, be directly compared with the QCD contributions $C_1^{(c/g^*)}$ which excludes $C_1^{(c/\gamma^*)}$ from $C_1^{(c)}$ in Eq. (3).

In the remainder of this paper, we use the same conventions of superscripts to other variables as those used in the short-distance coefficients $C_1^{(c)}$, $C_1^{(c/g^*)}$, $C_1^{(c\bar{c}gg)}$, $C_1^{(c\bar{c}g\gamma)}$, and $C_1^{(c/\gamma^*)}$. For example, $\Gamma^{(c)} = \Gamma[\Upsilon \to c + X]$ and $\Gamma^{(c\bar{c}gg)} = \Gamma[\Upsilon \to c\bar{c}gg]$.

B. Amplitude for $b\bar{b}$ annihilation into charm

The short-distance coefficients $C_1^{(c)}$, $C_1^{(c/g^*)}$, $C_1^{(c\bar{c}gg)}$, $C_1^{(c\bar{c}g\gamma)}$, and $C_1^{(c/\gamma^*)}$ are calculable by using perturbative matching, which involves the computation of the amplitudes for the corresponding perturbative short-distance processes such as $bb_1(^3S_1) \to c\bar{c}gg$. In this section, we summarize a way to calculate the annihilation amplitude for the process $bb_1(^3S_1) \to c\bar{c}gg$. Computations of the amplitudes for the remaining processes are analogous to that for $bb_1(^3S_1) \to c\bar{c}gg$.

At leading order in α_s, the short-distance process for $\Upsilon \to c + X$ is $b(p)\bar{b}(\bar{p}) \to c(p_1)\bar{c}(p_2)g(p_3)g(p_4)$ as shown in Fig. 1. The momenta of the b and the $\bar{b}$ can be expressed in terms of the total momentum P and the relative momentum q of the $b\bar{b}$ pair:

$$p = \tfrac{1}{2}P + q, \tag{6a}$$
$$\bar{p} = \tfrac{1}{2}P - q, \tag{6b}$$

where the p and the $\bar{p}$ satisfy the on-shell conditions $p^2 = \bar{p}^2 = m_b^2$ and $P \cdot q = 0$. In the rest frame of the $b\bar{b}$ pair, $P = (2E_b, \mathbf{0})$ and $q = (0, \mathbf{q})$, where $E_b = \sqrt{m_b^2 + \mathbf{q}^2}$. In general, the perturbative amplitude for the $b\bar{b}$ annihilation process is expressed as

$$\bar{v}(\bar{p})\mathcal{M}[b\bar{b}]u(p) = \mathrm{Tr}(\mathcal{M}[b\bar{b}]u(p)\bar{v}(\bar{p})), \tag{7}$$

where $\mathcal{M}[b\bar{b}]$ is a matrix that acts on spinors with both Dirac and color indices. The matrix $\mathcal{M}[b\bar{b}]$ for the short-distance process $b\bar{b} \to c(p_1)\bar{c}(p_2)g(p_3)g(p_4)$ is given by

$$\begin{aligned} \mathcal{M}[b\bar{b}] = {}& \frac{16\pi^2 \alpha_s^2}{(p_1 + p_2)^2} \bar{u}(p_1) T^a \gamma_\lambda v(p_2) \epsilon_{1\sigma}^{b*}(p_3) \epsilon_{2\tau}^{c*}(p_4) \\ & \times \sum_{\mathrm{perm}} [\gamma^\lambda \Lambda(p - p_3 - p_4) \\ & \times \gamma^\sigma \Lambda(p - p_4)\gamma^\tau \otimes T^a T^b T^c], \end{aligned} \tag{8}$$

where $\sum_{\mathrm{perm}}$ means the summation over the permutations of the three gluons attached to the bottom-quark line. T^a is a generator of the fundamental representation for the SU(3) color group and a, b, and c are color indices for the gluons. ϵ_1 and ϵ_2 are polarization vectors for the external gluons with momenta p_3 and p_4, respectively. Note that the expression in Eq. (8) is valid to any order in v. The function

$\Lambda(k)$ is defined by

$$\Lambda(k) = \frac{\slashed{k} + m_b}{k^2 - m_b^2}. \tag{9}$$

In general, the amplitude (7) contains contributions other than the color-singlet $b\bar{b}_1(^3S_1)$ state, which we want to project out. A convenient way to carry out the projection is to replace the spinor product $u(p)\bar{v}(\bar{p})$ in Eq. (7) by the direct product of the color-singlet projection operator π_1 and the spin-triplet projector $\epsilon_\mu \Pi_3^\mu$ [7,17,18], where

$$\pi_1 = \frac{1}{\sqrt{N_c}} \mathbb{1}, \tag{10a}$$

$$\Pi_3^\mu = -\frac{1}{4\sqrt{2}E_b(E_b + m_b)}(\slashed{p} + m_b)(\slashed{P} + 2E_b) \\ \times \gamma^\mu(\bar{\slashed{p}} - m_b), \tag{10b}$$

where $\mathbb{1}$ is the SU(3) color unit matrix and ϵ is the polarization four-vector of the $b\bar{b}_1(^3S_1)$ state so that $P \cdot \epsilon = 0$. The projectors (10) are normalized as $\text{Tr}[\pi_1 \pi_1^\dagger] = 1$ and $\text{Tr}[(\epsilon \cdot \Pi_3)(\epsilon \cdot \Pi_3)^\dagger] = 4p_0\bar{p}_0$. At leading order in v, the amplitude for the color-singlet spin-triplet S-wave $b\bar{b}$ pair can be written as $\epsilon_\mu \mathcal{A}_1^\mu[b\bar{b}_1(^3S_1)]$, where

$$\mathcal{A}_1^\mu = \text{Tr}(\mathcal{M}[b\bar{b}]\Pi_3^\mu \otimes \pi_1)|_{q=0}. \tag{11}$$

Because we are working in the leading order in v, we put $q = 0$ and, therefore, $E_b = m_b$.

The amplitude (11) is finite in the soft limits of any external gluons. At higher orders in v, infrared divergences arise in this S-wave amplitude while a P-wave amplitude has an infrared divergence at leading order in v. The amplitude (11) is sensitive to the ratio m_c/m_b. In the massless charm-quark limit $m_c/m_b \to 0$, the amplitude (11) acquires a collinear divergence, which cancels that arising from the charm-quark loop corrections to the gluon wave function for the $\Upsilon \to ggg$ process [14]. Because the amplitude (11) is free of any infrared and collinear divergences for $m_c \neq 0$ and $q = 0$, we do not need any regularization scheme and work in four space-time dimensions.

C. Short-distance coefficients

We proceed to calculate $C_1^{(c)}$ in the NRQCD factorization formula (2). The short-distance coefficient $C_1^{(c)}$ is insensitive to the long-distance nature of the Υ. Therefore, $C_1^{(c)}$ is calculable perturbatively. This can be done by perturbative matching [1,14]. In order to determine the short-distance coefficients $C_1^{(c)}$, we must calculate the annihilation rate for the color-singlet spin-triplet $b\bar{b}$ state by using perturbative QCD. The perturbative analog of the NRQCD factorization formula in Eq. (2) for the annihilation rate of the $b\bar{b}_1(^3S_1)$ pair is

$$d\Gamma[b\bar{b}_1(^3S_1) \to c + X] = dC_1^{(c)} \frac{\langle \mathcal{O}_1(^3S_1)\rangle_{b\bar{b}_1(^3S_1)}}{m_b^2}, \tag{12}$$

where the factorization formula (12) is written in a differential form. This form is useful for our purpose of calculating the momentum distribution of the charm quark.

1. Calculation of $C_1^{(c/g^*)}$

The differential annihilation rate of a color-singlet spin-triplet S-wave $b\bar{b}$ state into charm through the process $b\bar{b}_1(^3S_1) \to c\bar{c}gg$ can be expressed as

$$d\Gamma[b\bar{b}_1(^3S_1) \to c\bar{c}gg] = \left(\frac{1}{3}I_{\mu\nu}\sum_{c\bar{c}gg}\mathcal{A}_1^\mu \mathcal{A}_1^{\nu*}\right)\frac{d\Phi_4}{2!}, \tag{13}$$

where $\mathcal{A}_1$ is the perturbative amplitude (11) for $b\bar{b}_1(^3S_1) \to c\bar{c}gg$, $I^{\mu\nu}$ is the spin-1 polarization tensor for the $b\bar{b}_1(^3S_1)$,

$$I^{\mu\nu} = -g^{\mu\nu} + \frac{P^\mu P^\nu}{P^2}, \tag{14}$$

$d\Phi_4$ is the four-body phase space for $c\bar{c}gg$, and $\sum_{c\bar{c}gg}$ indicates summation over the spin states of $c\bar{c}gg$. The factor $1/3$ in Eq. (13) comes from averaging over the spin states for the $b\bar{b}_1(^3S_1)$. A factor of $1/2!$ is multiplied to the four-body phase space because there are two identical particles in the $c\bar{c}gg$ final state, whose phase spaces are integrated out.

In order to complete the matching calculation for $dC_1^{(c)}$, we need to compute the perturbative NRQCD matrix element:

$$\langle\mathcal{O}_1(^3S_1)\rangle_{b\bar{b}_1(^3S_1)} = 2N_c(2E_b)^2 = 8N_c m_b^2 + \mathcal{O}(v^2). \tag{15}$$

Substituting Eqs. (13) and (15) into Eq. (12) and multiplying by F_γ in order to take into account the $c\bar{c}g\gamma$ process as well as $c\bar{c}gg$, we find the differential short-distance coefficient $dC_1^{(c/g^*)}$:

$$dC_1^{(c/g^*)} = \frac{F_\gamma}{8N_c}\left(\frac{1}{3}I_{\mu\nu}\sum_{c\bar{c}gg}\mathcal{A}_1^\mu \mathcal{A}_1^{\nu*}\right)\frac{d\Phi_4}{2!}. \tag{16}$$

If we replace F_γ in Eq. (16) with unity or $F_\gamma - 1$, we get the expression for $dC_1^{(c\bar{c}gg)}$ or $dC_1^{(c\bar{c}g\gamma)}$, respectively.

A parametrization of the four-body phase space $d\Phi_4$ for the $c\bar{c}gg$ final state is derived in Appendix A:

$$d\Phi_4 = \frac{E_b^4}{2^{12}\pi^7} \\ \times \frac{r_Y(x_1^2 - r_c)^{1/2}\lambda^{1/2}(r_X^2, r_Y^2, r_c)}{r_X^2} dx_1 dr_Y d\Omega_2^* d\Omega_3^*, \tag{17}$$

where $\lambda(a, b, c) = a^2 + b^2 + c^2 - 2ab - 2bc - 2ca$. In Eq. (17), we have not set $v = 0$ so that the expression

can be used for a more general case. x_1, r_Y, and r_X in Eq. (17) are dimensionless variables defined by

$$x_1 = E_1/E_b, \tag{18a}$$

$$r_Y = m_Y/E_b, \tag{18b}$$

$$r_X = m_X/E_b, \tag{18c}$$

where E_1 is the energy of the charm quark in the rest frame of the $b\bar{b}$ pair and the invariant masses m_X and m_Y are defined by $m_X^2 = X^2 = (p_2 + p_3 + p_4)^2$ and $m_Y^2 = Y^2 = (p_3 + p_4)^2$, respectively. The ranges of the integration variables are

$$\sqrt{r_c} \leq x_1 \leq 1, \tag{19a}$$

$$0 \leq r_Y \leq \sqrt{4 - 4x_1 + r_c} - \sqrt{r_c}, \tag{19b}$$

where

$$r_c = m_c^2/E_b^2. \tag{20}$$

$d\Omega_2^*$ and $d\Omega_3^*$ are solid-angle elements of the charm antiquark with momentum p_2 in the X-rest frame and the gluon with momentum p_3 in the Y-rest frame, respectively.

2. Calculation of $C_1^{(c/\gamma^*)}$

The virtual-photon (γ^*) contribution $C_1^{(c/\gamma^*)}$ to the short-distance coefficient $C_1^{(c)}$ in Eq. (4) is proportional to that for the leptonic decay of the $\Upsilon(nS)$:

$$dC_1^{(\ell^+\ell^-)} = \frac{2\pi}{3} e_b^2 \alpha^2 \delta(1 - x_1) dx_1. \tag{21}$$

The short-distance coefficient $C_1^{(c/\gamma^*)}$ is

$$dC_1^{(c/\gamma^*)} = e_c^2 N_c \left(1 + \frac{r_c}{2}\right)\sqrt{1 - r_c} \times dC_1^{\ell^+\ell^-}$$

$$= \frac{\pi}{3} e_b^2 e_c^2 N_c \alpha^2 (2 + r_c)\sqrt{1 - r_c}\,\delta(1 - x_1) dx_1, \tag{22}$$

where the factor $\sqrt{1 - r_c}$ is the ratio of the phase space for the $c\bar{c}$ final state to the massless two-body phase space. The QED coupling $\alpha(\mu)$ in Eq. (22) is defined by the running coupling constant $\alpha(m_\Upsilon) = 1/131$, $1/130.9$, and $1/130.9$ for the radial quantum number $n = 1$, 2, and 3, respectively.

D. NRQCD matrix elements

In order to predict the decay widths (2) for the radial quantum numbers $n = 1$, 2, and 3, we must know the numerical value of $\langle \mathcal{O}_1 \rangle_\Upsilon$ for each state. In principle, the NRQCD matrix elements may be calculated in lattice simulations [19,20]. However, the only available NRQCD matrix element for an S-wave bottomonium is that for the $1S$ state [20]. Extrapolating the value in Ref. [20], which is obtained from an unquenched calculation using two dynamical light quarks, to three light-quark

flavors, one obtains $\langle \mathcal{O}_1 \rangle_{\Upsilon(1S)} = 3.95 \pm 0.43$ GeV^3, where we use the same extrapolation method that is given in Ref. [14].

The NRQCD matrix element $\langle \mathcal{O}_1 \rangle_\Upsilon$ may also be determined by comparing the NRQCD factorization formula for $\Gamma[\Upsilon \to e^+ e^-]$ with the empirical values, which are measured with uncertainties of order 2%. Recently, a method to resum a class of relativistic corrections to S-wave quarkonium processes has been developed [21,22], where order-α_s and resummed relativistic corrections are included in the NRQCD factorization formula for the leptonic decay width. This method has been used to determine the color-singlet NRQCD matrix elements for the S-wave charmonium states [22,23] and to the calculation of exclusive two-charmonium production in $e^+ e^-$ annihilation [24,25]. Using the method given in Ref. [22], we can determine the NRQCD matrix elements for each nS state:

$$\langle \mathcal{O}_1 \rangle_{\Upsilon(1S)} = 3.07^{+0.21}_{-0.19} \text{ GeV}^3, \tag{23a}$$

$$\langle \mathcal{O}_1 \rangle_{\Upsilon(2S)} = 1.62^{+0.11}_{-0.10} \text{ GeV}^3, \tag{23b}$$

$$\langle \mathcal{O}_1 \rangle_{\Upsilon(3S)} = 1.28^{+0.09}_{-0.08} \text{ GeV}^3. \tag{23c}$$

The uncertainties in the matrix elements in Eq. (23) reflect the errors in the lattice string tension, the one-loop pole mass of the bottom quark, the strong coupling constant, and the measured values for the leptonic widths as well as corrections of order v^2 that are not included in the potential model [22]. The central value of the matrix element (23a) for $\Upsilon(1S)$ is smaller than the lattice estimate by about 22%. In our numerical calculations, we use the values for the NRQCD matrix elements given in Eq. (23).

III. DECAY RATE

A. Charm-quark momentum distribution

In the quarkonium rest frame, the NRQCD factorization formula for the differential distribution with respect to the charm-quark energy fraction x_1 in Υ decay is easily deduced from Eq. (2):

$$\frac{d\Gamma^{(c)}}{dx_1} = \frac{dC_1^{(c)}}{dx_1} \frac{\langle \mathcal{O}_1 \rangle_\Upsilon}{m_b^2}, \tag{24}$$

where the differential coefficient is defined by $dC_1^{(c)} = dC_1^{(c/g^*)} + dC_1^{(c/\gamma^*)}$, which is analogous to Eq. (3), and $dC_1^{(c/g^*)}$ and $dC_1^{(c/\gamma^*)}$ are given in Eqs. (16) and (22). Integration over the variables dr_Y, $d\Omega_2^*$, and $d\Omega_3^*$ is implicit in $dC_1^{(c/g^*)}/dx_1$ on the right side of Eq. (24).

In the Υ rest frame, the magnitude of the three-momentum of the charm quark is determined by the energy fraction x_1 as Eq. (A11b). Using this relation, we obtain the charm-quark momentum distribution from Eq. (24). It is convenient to introduce the scaled momentum fraction y_1 that is defined as the momentum of the charm quark divided by the maximum value that is kinematically al-

lowed in Υ decay [14]. The physical range of the variable is simple: $0 < y_1 < 1$. By using the relations between x_1 and y_1

$$x_1 = \sqrt{(1 - r_c)y_1^2 + r_c}, \qquad (25a)$$

$$y_1 = \sqrt{\frac{x_1^2 - r_c}{1 - r_c}}, \qquad (25b)$$

we obtain the distribution for the scaled momentum fraction y_1:

$$\frac{d\Gamma^{(c)}}{dy_1} = \frac{(1 - r_c)y_1}{\sqrt{(1 - r_c)y_1^2 + r_c}} \frac{d\Gamma^{(c)}}{dx_1}, \qquad (26)$$

where $d\Gamma^{(c)}/dx_1$ is given in Eq. (24).

In the NRQCD factorization formula (24), the bottom-quark mass m_b appears in common for all three S-wave states. In order to be consistent with a preceding work [14], we use the one-loop pole mass $m_b = 4.6$ GeV for that m_b. The dimensionless short-distance coefficient $dC_1^{(c)}/dx_1$ depends on the strong coupling α_s and the ratio r_c. For the strong coupling, we use $\alpha_s(m_\Upsilon/2) = 0.215$, 0.212, and 0.210 for the radial quantum number 1, 2, and 3 of the Υ, respectively. The ratio r_c depends on m_c/E_b. In the non-relativistic limit $v \to 0$, which we are taking in this work, $r_c \to r \equiv (m_c/m_b)^2$. Then the bounds (19) of the variables x_1 and r_Υ are determined by r. We take $r_c = r = 4m_D^2/m_\Upsilon^2$, where $m_D = 1.87$ GeV is the average of the masses of the D^0 and D^+. For the S-wave spin-triplet bottomonium masses, we use $m_\Upsilon = 9.46$ GeV, 10.02 GeV, and 10.36 GeV, for the radial quantum number $n = 1$, 2, and 3, respectively [5]. This choice of r_c correctly reflects the physical kinematics [14]. We take the numerical values in Eq. (23) for the color-singlet NRQCD matrix elements.

Our theoretical prediction for the momentum distribution of the charm quark in the inclusive Υ decay is shown in Fig. 2 in terms of $d\Gamma^{(c/g^*)}/dy_1$, where the solid, dashed, and dotted lines are the distributions for the $1S$, $2S$, and $3S$ states, respectively. Because the color-singlet S-wave amplitudes for the processes are infrared finite, the distributions in Fig. 2 are finite over the whole range of y_1. This is different from those for $\chi_{bJ} \to c + X$ ($J = 0, 1, 2$), which grow rapidly as $y_1 \to 1$ [14]. The y_1 distributions are broad because of the four-body nature of the $c\bar{c}gg$ ($c\bar{c}g\gamma$) final state. The curves have the maximum values 2.44 keV at $y_1 = 0.51$, 1.38 keV at $y_1 = 0.50$, and 1.12 keV at $y_1 = 0.50$ for $\Upsilon(1S)$, $\Upsilon(2S)$, and $\Upsilon(3S)$, respectively.

As we have stated in Sec. II A, the distributions in Fig. 2 include only $b\bar{b}_1(^3S_1) \to c\bar{c}gg$ and $b\bar{b}_1(^3S_1) \to c\bar{c}g\gamma$ contributions to the short-distance coefficient $dC_1^{(c)}$ (16). For $y_1 < 1$, the leading virtual-photon contribution $\Upsilon \to \gamma^* \to c\bar{c}$ does not contribute because the distribution is proportional to $\delta(1 - y_1)$. The sharp peak from the virtual-photon contribution $d\Gamma^{(c/\gamma^*)}/dy_1$ at the end point has contributions
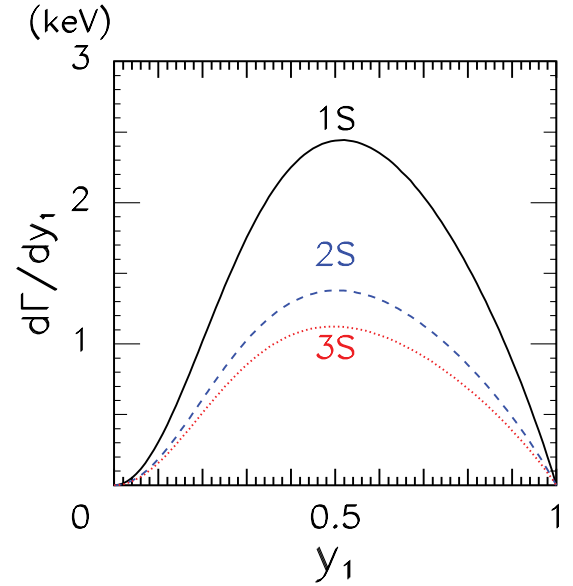

FIG. 2 (color online). Distributions of the scaled momentum fraction y_1 for the charm quark in decays of $\Upsilon(nS)$ for $n = 1$ (solid line), 2 (dashed line), and 3 (dotted line) by using $m_b = 4.6$ GeV, $\alpha_s(m_\Upsilon/2) = 0.215$, 0.212, and 0.210, and $\langle \mathcal{O}_1 \rangle_\Upsilon = 3.07$, 1.62, and 1.28 GeV^3 for the $1S$, $2S$, and $3S$ states, respectively. The distributions in the range $y_1 < 1$ are for the QCD contribution $d\Gamma^{(c/g^*)}$. There is a delta function at $y_1 = 1$ from the virtual-photon contribution $d\Gamma^{(c/\gamma^*)}$ in Eq. (22), which is not shown in this figure.

to the total inclusive charm production rate comparable to that of the QCD contributions illustrated in Fig. 2.

B. Total charm production rate

The inclusive charm production rate in Υ decay can be calculated by integrating the differential rate (24) over x_1 or the differential rate (26) over y_1. In Table I we list the partial widths $\Gamma^{(c/g^*)}$ and $\Gamma^{(c/\gamma^*)}$ and the total width $\Gamma^{(c)}$. The partial width $\Gamma^{(c/g^*)}$ for the QCD process is the sum of $\Gamma^{(c\bar{c}gg)}$ and $\Gamma^{(c\bar{c}g\gamma)}$, whose values can be obtained by multiplying $\Gamma^{(c/g^*)}$ by factors $F_\gamma^{-1} \approx 0.982$ and $1 - F_\gamma^{-1} \approx 0.0184$, respectively. The theoretical uncertainties in Table I are estimated as follows. We consider the uncertainties of the pole mass appearing in the factorization formula (2) as $m_b = 4.6 \pm 0.1$ GeV. As we have discussed

TABLE I. Inclusive charm production rate $\Gamma^{(c)}$ and partial widths $\Gamma^{(c/g^*)}$ and $\Gamma^{(c/\gamma^*)}$ in units of keV for $m_b = 4.6 \pm 0.1$ GeV and $\langle \mathcal{O}_1 \rangle_\Upsilon$ in Eq. (23). Uncertainties are estimated as stated in the text. The partial widths $\Gamma^{(c\bar{c}gg)}$ and $\Gamma^{(c\bar{c}g\gamma)}$ can be obtained by multiplying $\Gamma^{(c/g^*)}$ by factors $F_\gamma^{-1} \approx 0.982$ and $1 - F_\gamma^{-1} \approx 0.0184$, respectively.

State$Gamma$ (keV)	$\Gamma^{(c/g^*)}$	$\Gamma^{(c/\gamma^*)}$	$\Gamma^{(c)}$
$\Upsilon(1S)$	1.47 ± 0.36	2.60 ± 0.65	4.07 ± 0.75
$\Upsilon(2S)$	0.83 ± 0.20	1.38 ± 0.34	2.21 ± 0.40
$\Upsilon(3S)$	0.68 ± 0.16	1.09 ± 0.27	1.77 ± 0.32

TABLE II. Branching fractions $\mathrm{Br}^{(i)} = \Gamma^{(i)}/\Gamma[\Upsilon]$ for $(i) = (c/g^*)$, (c/γ^*), and (c), where $\Gamma^{(i)}$'s are given in Table I and $\Gamma[\Upsilon]$ is the measured total width [5] of Υ for radial quantum numbers $n = 1$, 2, and 3.

State\Br (%)	$\mathrm{Br}^{(c/g^*)}$	$\mathrm{Br}^{(c/\gamma^*)}$	$\mathrm{Br}^{(c)}$
$\Upsilon(1S)$	2.72 ± 0.67	4.81 ± 1.21	7.53 ± 1.39
$\Upsilon(2S)$	2.60 ± 0.67	4.30 ± 1.12	6.90 ± 1.37
$\Upsilon(3S)$	3.34 ± 0.87	5.36 ± 1.41	8.70 ± 1.74

earlier, the m_c dependence of the dimensionless short-distance coefficients are completely determined by $r_c = r = 4m_D^2/m_\Upsilon^2$. We do not vary r because the measured values for the hadron masses do not contribute to errors at the level of accuracy we take into account. We use the uncertainties in Eq. (23) for the NRQCD matrix elements. We consider the errors from uncalculated order-v^2 and order-α_s corrections by multiplying the central values shown in Table I by $v^2 \approx 10\%$ and by $\alpha_s(m_\Upsilon/2) \approx 0.215$, respectively. The error bars in the widths appearing in Table I are obtained by combining the uncertainties that are listed above in quadrature.

The branching fractions for the decay channels $c\bar{c}gg + c\bar{c}g\gamma$, $\gamma^* \to c\bar{c}$, and $c + X$ are listed in Table II. The numbers are obtained by dividing the numbers in Table I by the measured widths $\Gamma[\Upsilon(1S)] = 54.02 \pm 1.25$ keV, $\Gamma[\Upsilon(2S)] = 31.98 \pm 2.63$ keV, and $\Gamma[\Upsilon(3S)] = 20.32 \pm 1.85$ keV [5]. From Tables I and II, we conclude that the virtual-photon contribution is actually greater than the QCD contribution for all three S-wave states.

At the next-to-leading order in α_s, the virtual-photon contribution may contribute to the region $y_1 < 1$ because of real-gluon emissions. Because the leading-order contribution to $\Gamma^{(c/\gamma^*)}$ is greater than $\Gamma^{(c/g^*)}$ by about factors of 1.6–1.8, the order-α_s corrections to $\Gamma^{(c/\gamma^*)}$ may modify the shape of the y_1 distributions for $y_1 < 1$ by about 30%.

IV. CHARMED-HADRON MOMENTUM DISTRIBUTION

In Sec. III, we calculated the momentum distribution of the charm quark and the inclusive charm production rate in Υ decay. Since the charm quark hadronizes into one of the charmed hadrons with a probability of almost 100%, the charm production rate can be interpreted to be the sum of the production rates for the charmed hadrons h. The charmed hadrons include the D^0, D^+, D_s^+, and Λ_c^+, which are stable under strong and electromagnetic interactions, and excited charmed hadrons, whose decay product includes D^0, D^+, D_s^+, or Λ_c^+. As is discussed in Ref. [14], the momentum distribution of a charmed hadron produced in Υ decay is softer than that of the charm, because of the effect of hadronization. The momentum distribution for a charmed hadron h can be obtained by convolving the charm-momentum distribution with a fragmentation function for the charm quark to fragment into an h. For more

details, we refer the reader to Ref. [14] and references therein.

The fragmentation function $D_{c \to h}(z)$ gives the probability density for a charm quark with plus component of light-cone momentum $E_1 + p_1$ to hadronize into a charmed hadron h with light-cone momentum $E_h + p_h = z(E_1 + p_1)$. The fraction z can be expressed in terms of scaled light-cone momentum fractions z_1 for the charm and z_h for the charmed hadron, which are analogous to the scaled momenta y_1 and y_h [14], where z_1 is

$$z_1 = \frac{\sqrt{(1 - r_c)y_1^2 + r_c} + \sqrt{1 - r_c}\,y_1}{1 + \sqrt{1 - r_c}}. \qquad (27)$$

Then, the fraction z is expressed as

$$z = \frac{z_h}{z_1} \times \frac{(E_h + p_h)|_{\max}}{(E_1 + p_1)|_{\max}}, \qquad (28)$$

where the last factor on the right side of Eq. (28) becomes unity if the difference between the mass of the charm quark and that of the charmed hadron can be neglected. Within this approximation the momentum distribution of the charmed hadron can be written as [14]

$$\begin{aligned}
\frac{d\Gamma}{dy_h} &= \frac{dz_h}{dy_h} \int_{z_h}^1 \frac{dz_1}{z_1} D_{c \to h}(z_h/z_1) \frac{dy_1}{dz_1} \frac{d\Gamma}{dy_1} \\
&= \frac{\sqrt{1 - r_c}}{\sqrt{(1 - r_c)y_h^2 + r_c}} \int_{y_h}^1 dy_1 \\
&\quad \times \mathcal{D}_{c \to h}\left(\frac{\sqrt{(1 - r_c)y_h^2 + r_c} + \sqrt{1 - r_c}\,y_h}{\sqrt{(1 - r_c)y_1^2 + r_c} + \sqrt{1 - r_c}\,y_1} \right) \frac{d\Gamma}{dy_1}, \quad (29)
\end{aligned}$$

where $\mathcal{D}_{c \to h}(z) = z D_{c \to h}(z)$.

Explicit parametrizations for $D_{c \to h}(z)$ for some charmed hadrons h which are currently available can be found, for example, in Refs. [15,26]. Following a previous work on the charm production in the P-wave bottomonium decay [14], we refer to the results obtained by the Belle Collaboration [15]. They determined the optimal values of the parameters for analytic parametrizations of $D_{c \to h}(z)$ for various charmed hadrons by comparing their measured momentum distribution in $e^+ e^-$ annihilation near the center-of-momentum energy 10.6 GeV with the distributions predicted by Monte Carlo generators and fragmentation functions [15].

In our numerical analysis, we consider all the charmed hadrons considered in Ref. [15]. These cover all the channels being analyzed by the CLEO Collaboration: $\Upsilon(1S) \to h + X$, where $h = D^0$, D^+, D_s^+, D^{*+}, and Λ_c^+. We use the Kartvelishvili-Likhoded-Petrov (KLP) fragmentation function [27], which was used in the analysis of charmed-hadron momentum distribution in χ_b decays. The KLP fragmentation function has a simple parameterization depending only on the light-cone momentum fraction z:
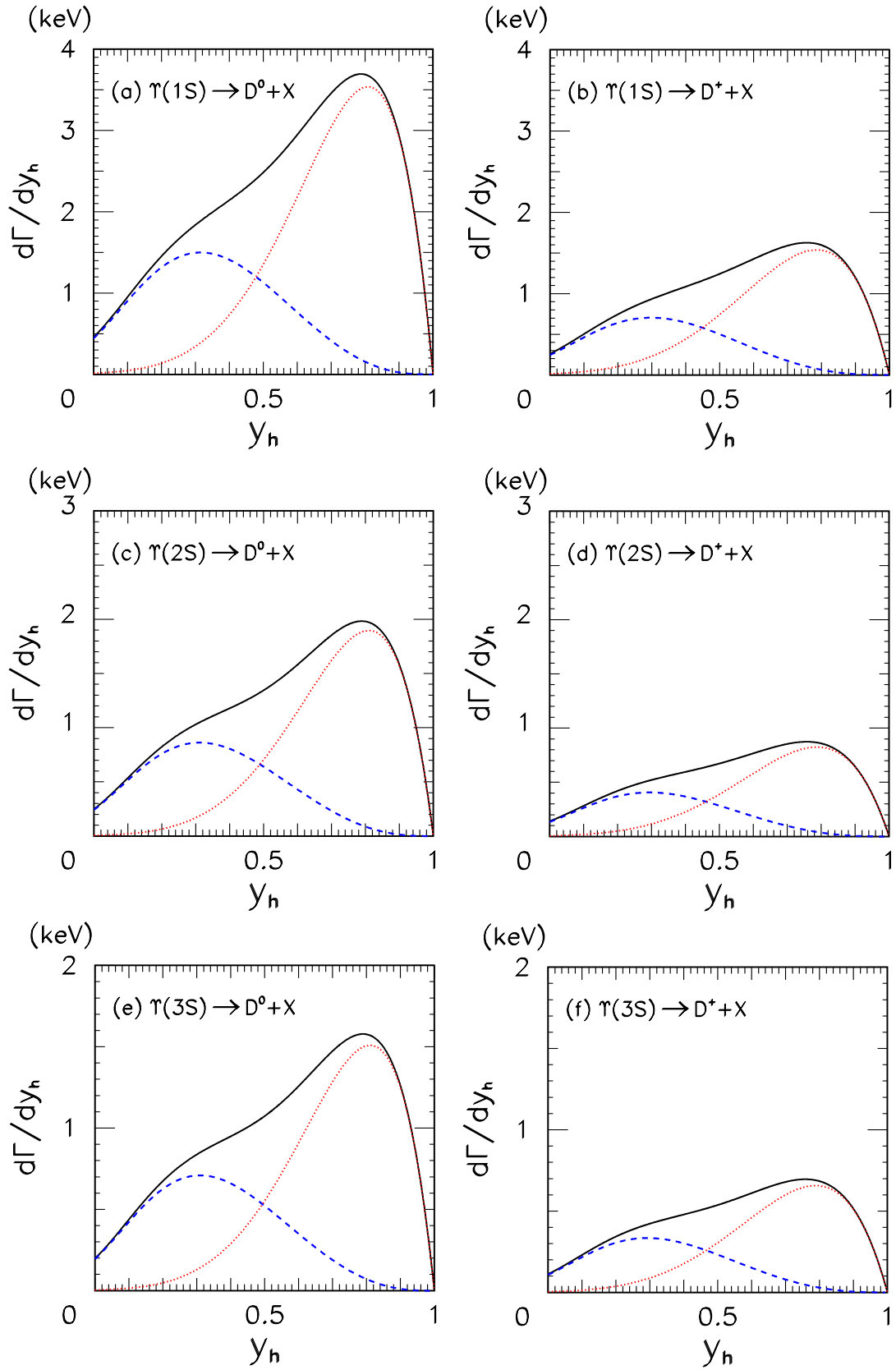
FIG. 3 (color online).   Distributions of the scaled momentum y_h in $\Upsilon(nS) \to h + X$ for $h = D^0$ (left column) and D^+ (right column) in units of keV. KLP parametrization is used for the charm fragmentation functions [15]. In each figure, solid, dashed, and dotted curves represent the total, QCD (c/g^*), and virtual-photon (c/γ^*) contributions, respectively.
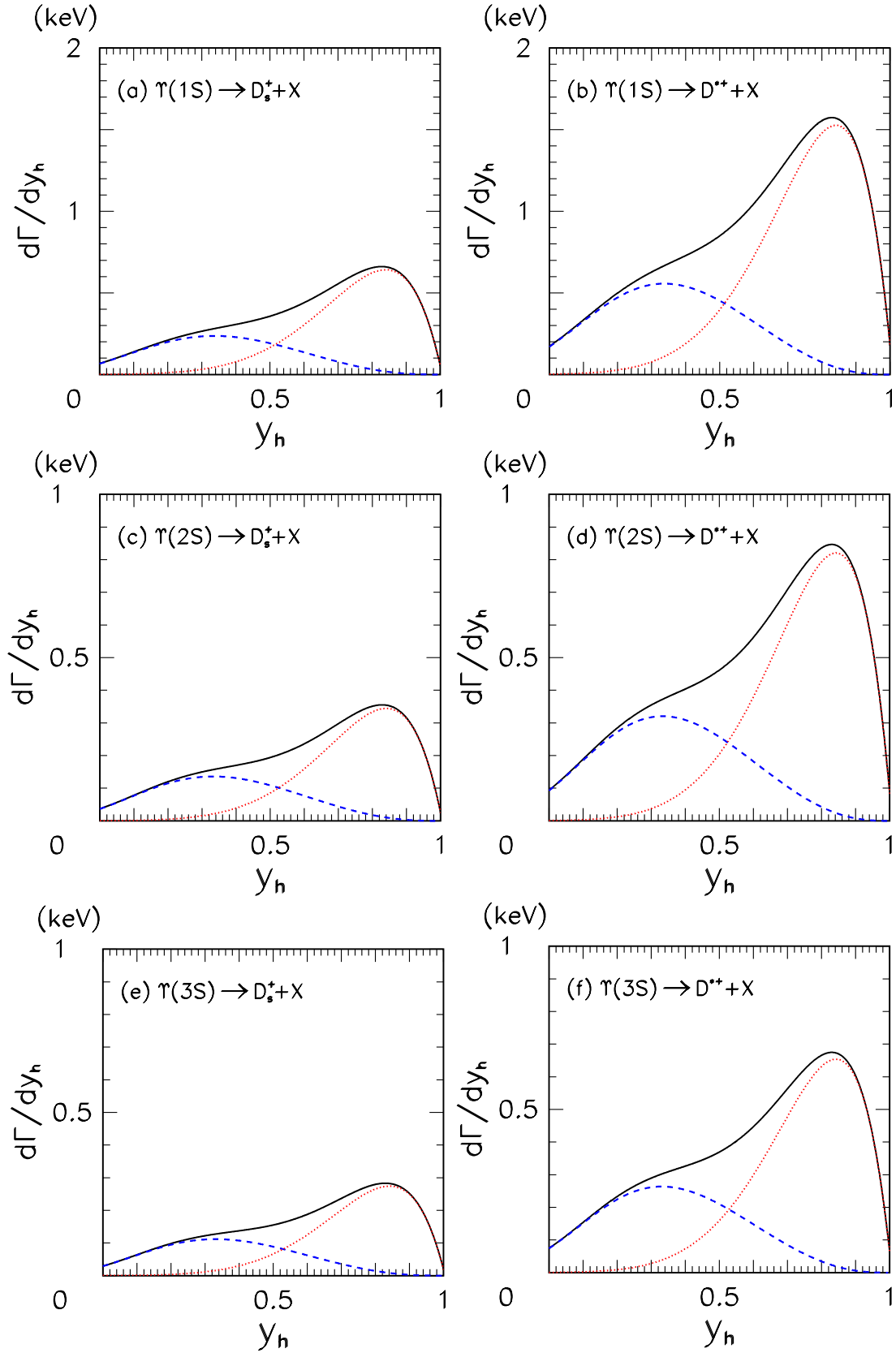
FIG. 4 (color online). Distributions of the scaled momentum y_h in $\Upsilon(nS) \to h + X$ for $h = D_s^+$ (left column) and D^{*+} (right column) in units of keV. KLP parametrization is used for the charm fragmentation functions [15]. In each figure, solid, dashed, and dotted curves represent the total, QCD (c/g^*), and virtual-photon (c/γ^*) contributions, respectively.

$$D_{c \to h}(z) = N_h z^{\alpha_c}(1 - z). \qquad (30)$$

The optimal values for the parameter α_c determined by the Belle Collaboration are $\alpha_c = 4.6, 4, 5.6, 5.6,$ and 3.6 for $D^0, D^+, D_s^+, D^{*+},$ and Λ_c^+, respectively [15].

The normalization N_h is determined by the constraint $\int_0^1 dz D_{c \to h}(z) = \text{Br}[c \to h]$. Using Table X of Ref. [15], one can infer that the inclusive fragmentation probabilities are $\text{Br}[c \to h] = 0.565, 0.268, 0.092, 0.220,$ and 0.075 for the $D^0, D^+, D_s^+, D^{*+},$ and Λ_c^+, respectively. As a result, we determine the normalization factors for various charmed hadrons as $N_{D^0} = 20.9, N_{D^+} = 8.04, N_{D_s^+} = 4.59, N_{D^{*+}} = 11.0,$ and $N_{\Lambda_c^+} = 1.93$. Note that the branching fractions for the $c \to D^0$ and $c \to D^+$ include feeddowns from higher resonances D^{0*} and D^{*+}. Substituting Eq. (30) into Eq. (29) and using the parameters listed above, we evaluate the momentum distributions for the charmed hadrons. In Eq. (29), we use $r_c = r = 4m_h^2/m_\Upsilon^2$ for z_h where $h = D_s^+, D^{*+},$ and Λ_c^+ while $r_c = r = 4m_D^2/m_\Upsilon^2$ for z_1 and z_D where $D = D^0$ and D^+. We use $m_{D_s^+} = 1.97$ GeV, $m_{D^{*+}} = 2.01$ GeV, and $m_{\Lambda_c^+} = 2.29$ GeV [5].

In Fig. 3, we show the scaled momentum y_h distributions of the charmed hadrons in the decays $\Upsilon(nS) \to h + X$, where $h = D^0$ (left column) and D^+ (right column) for radial quantum numbers $n = 1, 2,$ and 3. The distributions for $\Upsilon(nS) \to h + X$, where $h = D_s^+$ (left column) and D^{*+} (right column) are illustrated in Fig. 4 and those for the Λ_c^+ baryon in Fig. 5. In Figs. 3–5, the dotted and dashed curves represent the virtual-photon and QCD contributions, respectively. The solid lines are the sums of the two contributions. In contrast to the charm-quark momentum distribution, which has a virtual-photon contribution only at the end point $y_1 = 1$, the virtual-photon contribution for a charmed hadron is smeared out to the region $y_h < 1$. The peaks of the virtual-photon, QCD, and total contributions are placed in the ranges $0.78 < y_h < 0.84$, $0.28 < y_h < 0.34$, and $0.75 < y_h < 0.83$, respectively. The softening of the QCD contribution can be seen by comparing the QCD contribution to the charmed-hadron momentum distributions in Figs. 3–5 with the charm-quark momentum distributions in Fig. 2. The softening of the virtual-photon contribution is even more dramatic, transforming a delta function at $y_1 = 1$ into the virtual-photon contributions in Figs. 3–5. Hadronization significantly softens the momentum spectrum of charmed hadrons.

The charmed-hadron production rates in Υ decay are obtained by integrating over y_h in Eq. (29) for each hadron. The rates are the same as the area under the solid lines in Figs. 3–5. The production rates of $D^0, D^+, D_s^+, D^{*0},$ and Λ_c^+ in $\Upsilon(1S)$ decay are 2.25 keV, 1.06 keV, 0.37 keV, 0.87 keV, and 0.28 keV, respectively, where the contributions of the virtual-photon processes amount to about 68–69% of the production rates. In $\Upsilon(2S)$ decay, we get 1.23 keV, 0.58 keV, 0.20 keV, 0.47 keV, and 0.15 keV for each hadron production rate, respectively, while in $\Upsilon(3S)$
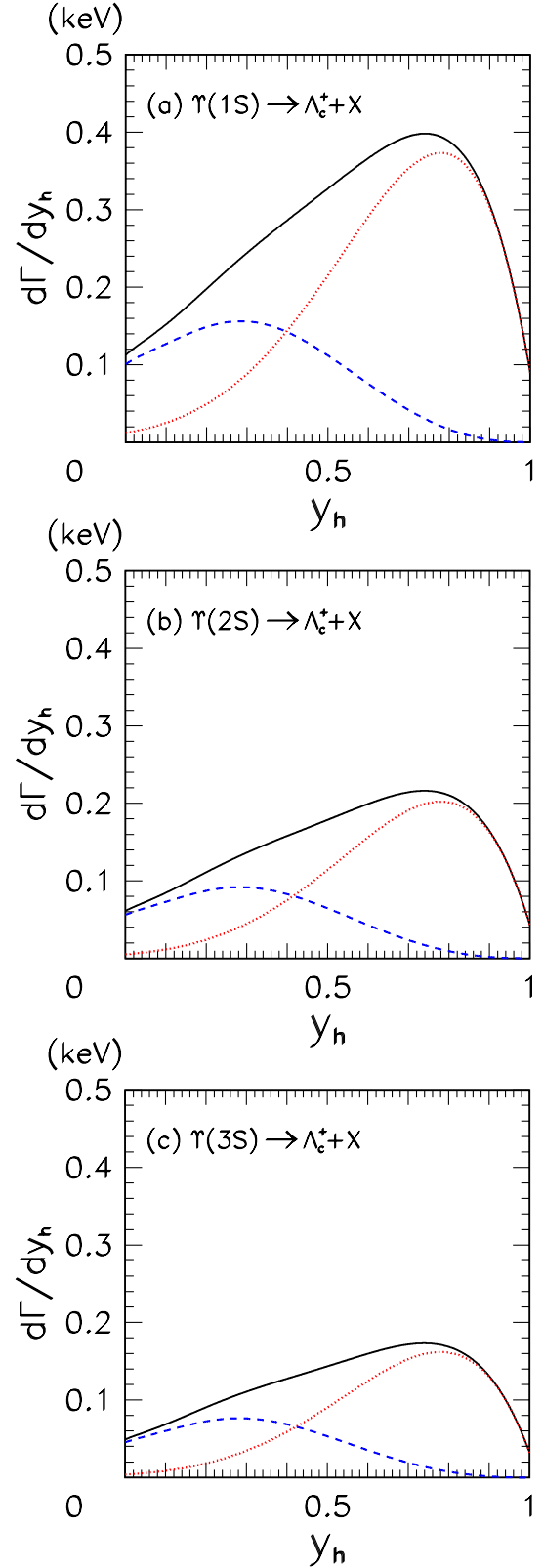

FIG. 5 (color online). Distributions of the scaled momentum y_h in $\Upsilon(nS) \to \Lambda_c^+ + X$ in units of keV. KLP parametrization is used for the charm fragmentation functions [15]. In each figure, solid, dashed, and dotted curves represent the total, QCD (c/g^*), and virtual-photon (c/γ^*) contributions, respectively.

decay, 0.98 keV, 0.46 keV, 0.16 keV, 0.38 keV, and 0.12 keV, respectively. For the decays of the 2S state into charmed hadrons the virtual-photon contributions add up to about 63%–67% while for those of the 3S state to about 63%–66%. The fractions of the virtual-photon contributions decrease up to about 63% as the radial quantum number n of the $\Upsilon(nS)$ increases. If we compare the momentum distributions of charmed hadrons with that of the charm quark, we could observe that hadronization softens the distributions. For the QCD contributions, whose charm-quark distribution reaches lower end point, the vertical-axis intercepts for the charmed-hadron momentum distributions significantly shift to the positive direction. This results in loss of probability. Because the loss is minor for the virtual-photon contributions, whose charm-quark distributions are concentrated at $y_1 = 1$, the fractions of the virtual-photon contributions in the charmed-hadron production rates are greater than that of the charm-quark production rate. As is discussed in Ref. [14], this change in normalization is of order r, which is at the level of the error in the fragmentation approximation itself, which is derived from QCD by neglecting corrections on the order of the square of the quark mass divided by the hard-scattering momentum [28].

As we show in Fig. 3, the production rate of D^0 is more than twice as large as that of D^+. This reflects the fact that the D^0 may be produced from the decays of D^{*0} and D^{*+} while D^+ has the contribution only from the feeddown from the decay of D^{*+} besides direct production from the charm quark. As we show in Fig. 5, the shape of the scaled momentum distribution of the Λ_c^+ is broader than that of the other charmed hadrons. Because Λ_c^+ is the heaviest among the charmed hadrons that we consider, the smearing effects from hadronization is most significant in Λ_c^+ production.

There are uncertainties in the fragmentation function. Part of the uncertainties can be estimated by comparing the results shown above with those obtained by using different parametrizations for the fragmentation functions. We also carried out the same calculations by using the Collins-Spiller (CS) fragmentation functions [29] whose parameters are determined in Ref. [15]. With the CS fragmentation functions, the heights of the peaks are smaller than those from the KLP fragmentation functions by about 8%. This difference is small enough to be within our theoretical uncertainties of about 20%. Another important source of the uncertainties may come from the Monte Carlo. The estimate of the uncertainties is out of the scope of this work.

V. SUMMARY

We have studied inclusive charm production in the decay of the spin-triplet bottomonium state $\Upsilon(nS)$ based on the color-singlet mechanism of the NRQCD factorization formalism. The branching fractions of the $\Upsilon(nS)$ into

charm are predicted to be $(7.5 \pm 1.4)\%$, $(6.9 \pm 1.4)\%$, and $(8.7 \pm 1.7)\%$ for $n = 1$, 2, and 3, respectively. The dominant contribution comes from the virtual-photon process $b\bar{b}_1(^3S_1) \to \gamma^* \to c\bar{c}$, which contributes about 60% of the partial width for inclusive charm production in each $\Upsilon(nS)$ decay. The remaining portion of the partial width comes from the QCD contribution, which is dominated by $b\bar{b}_1(^3S_1) \to ggg^*$ followed by $g^* \to c\bar{c}$. The $b\bar{b}_1(^3S_1) \to c\bar{c}g\gamma$ diagrams contribute only about 0.7% of the total widths of $\Upsilon(nS)$ into charm.

We have also presented the momentum distribution of the charm quark in the $\Upsilon(nS)$ decays. The virtual-photon contribution is localized at the end point $(y_1 = 1)$. The QCD contributions, which have four-body final states, are broad and have peaks near $y_1 = 0.5$. By convolving the charm-momentum distribution with the fragmentation function $D_{c \to h}(z)$ that have been fit to the e^+e^- annihilation data by the Belle Collaboration, we have computed the momentum distribution of charmed hadrons $h = D^0$, D^+, D_s^+, D^{*+}, and Λ_c^+ produced in $\Upsilon(nS) \to h + X$. The resulting momentum distributions of the charmed hadrons are significantly softer than that of the charm quark. The large virtual-photon contribution, which is localized at the end point $(y_1 = 1)$ for the charm quark, is smeared out into a distribution with a peak near $y_h \approx 0.8$. The order-α_s corrections to the virtual-photon contributions may enhance the charm-quark momentum distribution in the range $y_1 < 1$. The cancellation of the infrared divergence at that order may produce a singular distribution at the end point, which is similar to that of the P-wave decays.

In a recent analysis being carried out by the CLEO Collaboration, as a part of measurement, the virtual-photon contribution is subtracted from the data. In order to facilitate comparison with the experimental data, we have provided all the predictions separately for the QCD, virtual-photon, and total contributions. Comparison with the experimental results will test the leading-order approximations employed in this work.

APPENDIX: THE FOUR-BODY PHASE SPACE

The four-body phase space $d\Phi_4$ is defined by

$$d\Phi_4 = (2\pi)^4 \delta^{(4)}\left(P - \sum_{i=1}^{4} p_i\right) \prod_{i=1}^{4} \frac{d^3 p_i}{(2\pi)^3 2E_i}, \quad \text{(A1)}$$

where E_i and p_i are the energy and momentum of the particle i in the final state. For $Y(P) \to c(p_1)\bar{c}(p_2)g(p_3)g(p_4)$, $p_1^2 = p_2^2 = m_c^2$, $p_3^2 = p_4^2 = 0$, and $\sqrt{P^2} = 2E_b$. Since we are interested in the momentum distribution of the charm quark in the P-rest frame, we evaluate $d\Phi_4$ leaving the three-momentum p_1 unintegrated:

$$d\Phi_4 = \frac{d^3 p_1}{(2\pi)^3 2E_1} d\Phi_3(X \to p_2 + p_3 + p_4), \quad \text{(A2)}$$

where $X = P - p_1$. The three-body phase space $d\Phi_3(X \to p_2 + p_3 + p_4)$ can be expressed as a chain of two-body phase spaces:

$$d\Phi_3(X \to p_2 + p_3 + p_4)$$
$$= d\Phi_2(X \to p_2 + Y)\frac{dm_Y^2}{2\pi} d\Phi_2(Y \to p_3 + p_4), \quad \text{(A3)}$$

where $Y = p_3 + p_4$ and m_Y is the invariant mass of Y. When a squared amplitude is summed over spin states of all the particles in both initial and final states, the squared amplitude becomes independent of the solid angle of p_1. Integrating over the solid angle of p_1, substituting Eq. (A3) into Eq. (A2), and expressing the two-body phase spaces $d\Phi_2(X \to p_2 + Y)$ and $d\Phi_2(Y \to p_3 + p_4)$ in the X and Y rest frames, respectively, we find that

$$d\Phi_4 = \frac{|p_1||p_2^*||p_3^*|}{2^{10}\pi^7 m_X} dE_1 dm_Y d\Omega_2^* d\Omega_3^*, \quad \text{(A4)}$$

where $m_X = (4E_b^2 - 4E_b E_1 + m_c^2)^{1/2}$ is the invariant mass of X. The ranges of the integration variables E_1 and m_Y are given by

$$m_c \le E_1 \le E_b, \quad \text{(A5a)}$$
$$0 \le m_Y \le m_X - m_c. \quad \text{(A5b)}$$

In Eq. (A4), $|p_1|$ and E_1 are the absolute value of the charm-quark momentum and energy in the P-rest frame while p_2^* (p_3^*) and $d\Omega_2^*$ ($d\Omega_3^*$) are the three-momentum and the solid-angle element of the $\bar{c}(g)$ in the $X(Y)$-rest frame, respectively. Explicit components of the four-vectors p_1, p_2^*, and p_3^* are

$$p_1 = (E_1, 0, 0, |p_1|), \quad \text{(A6a)}$$
$$p_2^* = (E_2^*, |p_2^*|\sin\theta_2^*\cos\phi_2^*, |p_2^*|\sin\theta_2^*\sin\phi_2^*, |p_2^*|\cos\theta_2^*), \quad \text{(A6b)}$$
$$p_3^* = (|p_3^*|, |p_3^*|\sin\theta_3^*\cos\phi_3^*, |p_3^*|\sin\theta_3^*\sin\phi_3^*, |p_3^*|\cos\theta_3^*), \quad \text{(A6c)}$$

where (θ_2^*, ϕ_2^*) and (θ_3^*, ϕ_3^*) are the polar and azimuthal angles of p_2^* and p_3^* in the X-rest and Y-rest frame, respectively. In Eq. (A6),

$$E_2^* = \frac{m_X^2 + m_c^2 - m_Y^2}{2m_X}, \quad \text{(A7a)}$$

$$|p_1| = (E_1^2 - m_c^2)^{1/2}, \quad \text{(A7b)}$$

$$|p_2^*| = \frac{1}{2m_X} \lambda^{1/2}(m_X^2, m_Y^2, m_c^2), \quad \text{(A7c)}$$

$$|p_3^*| = \frac{m_Y}{2}, \quad \text{(A7d)}$$

where $\lambda(a, b, c) = a^2 + b^2 + c^2 - 2ab - 2bc - 2ca$. Note that in Eq. (A6) p_2^* and p_3^* are given in the X-rest and Y-rest frame while in order to evaluate Eq. (16) it is convenient to express them in the P-rest frame. We introduce the boost matrix $\Lambda^\mu_{\ \nu}$ transforming an arbitrary vector $k^* = (\sqrt{k^2}, 0)$ into $k = (k^0, \mathbf{k})$:

$$k^\mu = \Lambda^\mu_{\ \nu} k^{*\nu}, \quad \text{(A8a)}$$

$$\Lambda^0_{\ 0} = \frac{k^0}{\sqrt{k^2}}, \quad \text{(A8b)}$$

$$\Lambda^0_{\ i} = \Lambda^i_{\ 0} = \frac{k^i}{\sqrt{k^2}}, \quad \text{(A8c)}$$

$$\Lambda^i_{\ j} = \delta^{ij} + \frac{k^0 - \sqrt{k^2}}{\sqrt{k^2}} \frac{k^i k^j}{|\mathbf{k}|^2}, \quad \text{(A8d)}$$

where $i, j = 1, 2, 3$. The explicit components of p_2 are obtained by boosting p_2^* from the X-rest frame to the P-rest frame, where $\Lambda^\mu_{\ \nu}$ is determined by substituting X into k in Eq. (A8). To obtain p_3, we need two steps. First, we boost p_3^* from the Y-rest frame to the X-rest frame where the boost matrix is given by replacing k in Eq. (A8) by Y. The components of Y in the X-rest frame are easily obtained by using $Y = X - p_2$ valid in any frame. Let the obtained four-vector be p_3^X. It is easy to obtain p_3 by boosting p_3^X from the X-rest frame to the P-rest frame. Now we can express all the momenta in the P-rest frame so that the Lorentz scalars in Eq. (16) can be represented in the P-rest frame.

It is convenient to introduce dimensionless variables x_1 and r_Y defined by

$$x_1 = E_1/E_b, \quad \text{(A9a)}$$
$$r_Y = m_Y/E_b, \quad \text{(A9b)}$$

where the ranges of the variables are

$$\sqrt{r_c} \le x_1 \le 1, \quad \text{(A10a)}$$
$$0 \le r_Y \le \sqrt{4 - 4x_1 + r_c} - \sqrt{r_c}. \quad \text{(A10b)}$$

r_c is the square of the ratio of the charm-quark mass and E_b, $r_c = m_c^2/E_b^2$. The energy and momenta E_2^*, $|\boldsymbol{p}_1|$, $|\boldsymbol{p}_2^*|$, and $|\boldsymbol{p}_3^*|$ are expressed in terms of the variables x_1 and r_Y:

$$E_2^* = \frac{E_b}{2r_X}(r_X^2 - r_Y^2 + r_c), \quad \text{(A11a)}$$

$$|\boldsymbol{p}_1| = E_b(x_1^2 - r_c)^{1/2}, \quad \text{(A11b)}$$

$$|\boldsymbol{p}_2^*| = \frac{E_b}{2r_X}\lambda^{1/2}(r_X^2, r_Y^2, r_c), \quad \text{(A11c)}$$

$$|\boldsymbol{p}_3^*| = \frac{r_Y}{2}E_b, \quad \text{(A11d)}$$

where $r_X = m_X/E_b$. Substituting Eqs. (A9) and (A11) into Eq. (A4), we obtain the four-body phase space $d\Phi_4$ in terms of x_1 and r_Y:

$$d\Phi_4 = \frac{E_b^4}{2^{12}\pi^7}$$
$$\times \frac{r_Y(x_1^2 - r_c)^{1/2}\lambda^{1/2}(r_X^2, r_Y^2, r_c)}{r_X^2}dx_1 dr_Y d\Omega_2^* d\Omega_3^*.$$
$$\text{(A12)}$$

[1] G. T. Bodwin, E. Braaten, and G. P. Lepage, Phys. Rev. D **51**, 1125 (1995); **55**, 5853(E) (1997).

[2] W. E. Caswell, G. P. Lepage, and J. R. Sapirstein, Phys. Rev. Lett. **38**, 488 (1977).

[3] P. B. Mackenzie and G. P. Lepage, Phys. Rev. Lett. **47**, 1244 (1981).

[4] J. Campbell, F. Maltoni, and F. Tramontano, Phys. Rev. Lett. **98**, 252002 (2007).

[5] W. M. Yao *et al.* (Particle Data Group), J. Phys. G **33**, 1 (2006).

[6] W. Y. Keung and I. J. Muzinich, Phys. Rev. D **27**, 1518 (1983).

[7] G. T. Bodwin and A. Petrelli, Phys. Rev. D **66**, 094011 (2002).

[8] K. M. Cheung, W. Y. Keung, and T. C. Yuan, Phys. Rev. D **54**, 929 (1996).

[9] F. Maltoni and A. Petrelli, Phys. Rev. D **59**, 074006 (1999).

[10] N. Brambilla, X. Garcia i Tormo, J. Soto, and A. Vairo, Phys. Rev. D **75**, 074014 (2007).

[11] H. Fritzsch and K. H. Streng, Phys. Lett. B **77**, 299 (1978).

[12] I. I. Y. Bigi and S. Nussinov, Phys. Lett. B **82**, 281 (1979).

[13] H. Albrecht *et al.* (ARGUS Collaboration), Z. Phys. C **55**, 25 (1992).

[14] G. T. Bodwin, E. Braaten, D. Kang, and J. Lee, Phys. Rev. D **76**, 054001 (2007).

[15] R. Seuster *et al.* (Belle Collaboration), Phys. Rev. D **73**, 032002 (2006).

[16] R. Briere (private communication).

[17] J. H. Kuhn, J. Kaplan, and E. G. O. Safiani, Nucl. Phys. **B157**, 125 (1979).

[18] B. Guberina, J. H. Kuhn, R. D. Peccei, and R. Ruckl, Nucl. Phys. **B174**, 317 (1980).

[19] G. T. Bodwin, D. K. Sinclair, and S. Kim, Phys. Rev. Lett. **77**, 2376 (1996).

[20] G. T. Bodwin, D. K. Sinclair, and S. Kim, Phys. Rev. D **65**, 054504 (2002).

[21] G. T. Bodwin, D. Kang, and J. Lee, Phys. Rev. D **74**, 014014 (2006).

[22] G. T. Bodwin, H. S. Chung, D. Kang, J. Lee, and C. Yu, arXiv:0710.0994.

[23] H. S. Chung, J. Lee, and C. Yu, J. Korean Phys. Soc. **50**, 357 (2007).

[24] G. T. Bodwin, D. Kang, T. Kim, J. Lee, and C. Yu, AIP Conf. Proc. **892**, 315 (2007).

[25] G. T. Bodwin, J. Lee, and C. Yu, arXiv:0710.0995.

[26] M. Artuso *et al.* (CLEO Collaboration), Phys. Rev. D **70**, 112001 (2004).

[27] V. G. Kartvelishvili, A. K. Likhoded, and V. A. Petrov, Phys. Lett. B **78**, 615 (1978).

[28] J. C. Collins, D. E. Soper, and G. Sterman, Adv. Ser. Dir. High Energy Phys. **5**, 1 (1988).

[29] P. D. B. Collins and T. P. Spiller, J. Phys. G **11**, 1289 (1985).